Size-dependent exciton *g* factor in self-assembled InAs/InP quantum dots

N. A. J. M. Kleemans,* J. van Bree, M. Bozkurt, P. J. van Veldhoven, P. A. Nouwens, R. Nötzel, A. Yu. Silov, and P. M. Koenraad

Photonics and Semiconductor Nanophysics, COBRA, Eindhoven University of Technology, P.O. Box 513, NL-5600 MB Eindhoven, The Netherlands

M. E. Flatté

Department of Physics and Astronomy and Optical Science and Technology Center, University of Iowa, Iowa City, Iowa 52242, USA

(Received 15 October 2008; revised manuscript received 10 December 2008; published 16 January 2009)

We have studied the size dependence of the exciton *g* factor in self-assembled InAs/InP quantum dots. Photoluminescence measurements on a large ensemble of these dots indicate a multimodal height distribution. Cross-sectional scanning tunneling microscopy measurements have been performed and support the interpretation of the macrophotoluminescence spectra. More than 160 individual quantum dots have systematically been investigated by analyzing single dot magnetoluminescence between 1200 and 1600 nm. We demonstrate a strong dependence of the exciton *g* factor on the height and diameter of the quantum dots, which eventually gives rise to a sign change of the *g* factor. The observed correlation between exciton *g* factor and the size of the dots is in good agreement with calculations. Moreover, we find a size-dependent anisotropy splitting of the exciton emission in zero magnetic field.

DOI: 10.1103/PhysRevB.79.045311 PACS number(s): 78.20.Ls, 71.70.Ej, 73.21.La

I. INTRODUCTION

Self-assembled quantum dots are one of the most promising candidates to be used as building blocks in quantum information processing.[1–4] For instance, single-qubit operations have been proposed by changing the local effective Zeeman interaction in a quantum dot.[5,6] Control over the exciton *g* factor (g_{ex}), defined by Eq. (2), is thus highly desirable for the realization of individual qubits.[7] Moreover, a sign change of the exciton *g* factor is very desirable in quantum information processing and thus there is a strong interest in quantum dots having a zero *g* factor due to the structure of the dot. To investigate the size, shape, and composition dependence of the electron, hole, and exciton *g* factor, theoretical investigations using the $\mathbf{k}\cdot\mathbf{p}$ approximation[8–10] as well as tight-binding calculations[11,12] have been performed on InAs/GaAs dots. The self-assembly process of quantum dots gives rise to a distribution in size, shape, and composition of the dots and therefore leads to a dot to dot variation in g_{ex}. This opens the possibility of utilizing the growth conditions to engineer g_{ex}.[13] However, up to now experiments on InAs/GaAs QDs did not reveal a strong correlation between emission energy and g_{ex}.[9,14]

We have performed photoluminescence (PL) measurements on a large number of single InAs/InP quantum dots in order to investigate the energy dependence of g_{ex} and its dependence on the structural properties of individual quantum dots. In this paper we will demonstrate strong correlations between g_{ex}, the diamagnetic shift, and the emission energy of the InAs/InP quantum dots. Eventually, the size dependence of g_{ex} will lead to a sign change of g_{ex}. The observed correlations can be explained well by the theoretical trends discussed in Ref. 10. Furthermore, we will analyze the anisotropy splitting of these dots and correlate this to the height and lateral size of the dots. As the PL of the InAs/InP quantum dots is tunable to 1.55 μm,[15–18] our results show that *g* factor engineering is also feasible at telecommunication wavelengths.

II. SAMPLE GROWTH AND CHARACTERIZATION

A. Growth

Our quantum dots are grown by metal-organic vapor-phase epitaxy (MOVPE). A layer of 100 nm of InP has been grown on a *n*-doped InP (100) substrate with a 2° miscut toward the [110] direction. Two monolayers (ML) of GaAs were deposited as an interlayer, thereby reducing the As/P exchange reaction. On top of this interlayer a 2 ML InAs layer is grown, resulting in the formation of quantum dots. The quantum dot layer is capped by 200 nm of InP. For atomic force microscopy (AFM) a layer of surface quantum dots was grown under the same conditions. From the AFM measurements we find an average height of the dots of 2 ± 1 nm and a dot diameter of 34 ± 5 nm. More details about the growth of these wavelength-tunable InAs quantum dots in InP can be found in Ref. 16.

B. Macrophotoluminescence

The sample is characterized by temperature-dependent PL measurements performed on a large ensemble of dots. The quantum dots are excited by a laser operating at 532 nm and with a spot size of ~4 mm^2. The macro-PL is detected by an InGaAs array detector up to 1550 nm and with an InSb single-channel detector above 1400 nm. The spectra taken at different temperatures are shown in Fig. 1. These spectra are plotted by matching at 1450 nm the spectra obtained by both detectors. Instead of a single Gaussian distribution, characteristic for highly homogeneous quantum dots, a series of peaks ($P1-P9$) is observed. The spectrum at $T=4.5$ K displays strong similarities with the ones reported in Refs. 19 and 20; the peaks were identified as quantum dots with discrete height differences of 1 ML and the dots were modeled accordingly. In the same way we attribute the different peaks to a multimodal height distribution of our dots. Quantum

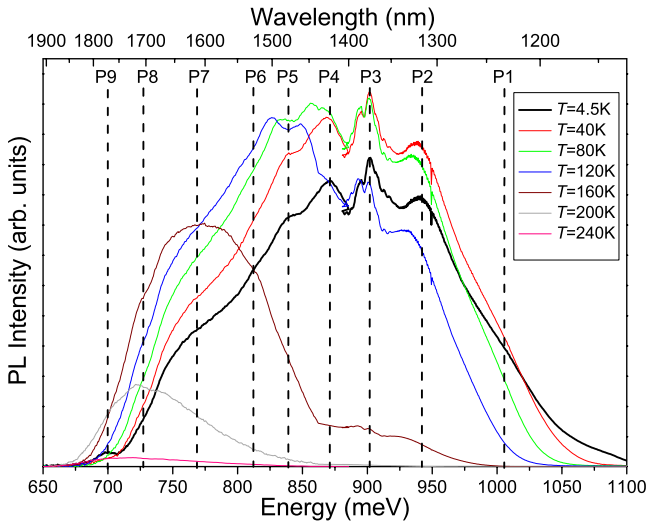

FIG. 1. (Color online) PL spectra of a large ensemble of quantum dots measured at different temperatures. A multiple peak structure is observed consisting of nine peaks. The peak positions at $T=4.5$ K are indicated by the dotted lines. We attribute the multiple peak structure to the multimodal height distribution of the dots. Quantum dots having the smallest height have luminescence around peak $P1$.

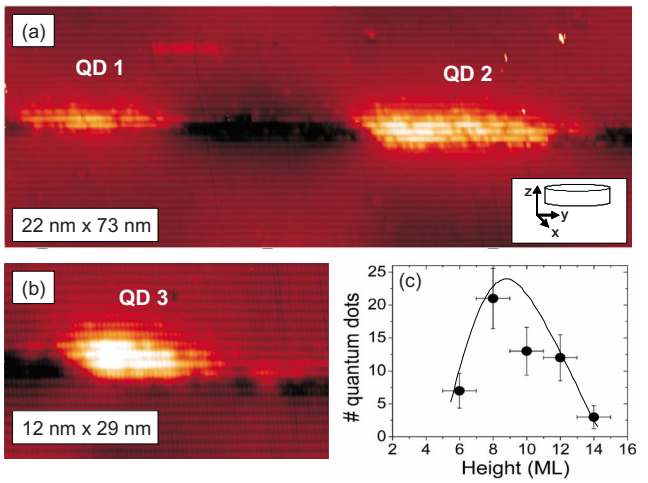

FIG. 2. (Color online) X-STM characterization of InAs/InP quantum dots of (a) 3 BL (6 ± 1 ML), 5 BL (10 ± 1 ML), and (b) 4 BL (8 ± 1 ML) heights. The bright contrast corresponds to InAs, whereas the dark contrast corresponds to GaAs. The distribution of the different heights of the dots is given in (c). The inset of (a) shows the typical disk shape of our dots.

dots emitting around $P9$ at the low-energy side of the spectrum have the largest height, whereas dots emitting at the high-energy side have the smallest height. The width of the peaks is due to the dot to dot variation in the diameter and composition. The structure present in peak $P3$ is still not understood. A redistribution of carriers over the dots having different heights occurs for increasing temperatures. At elevated temperatures the excitons in the QDs with smaller height can escape and diffuse toward the higher dots, where they are captured and recombine.

C. Cross-sectional scanning tunneling microscopy

To characterize the dot size, shape, and composition we performed cross-sectional scanning tunneling microscopy (X-STM), as was done on similar dots recently.[21] The measurements have been performed in constant current mode. Three different quantum dots are shown in Figs. 2(a) and 2(b). The images were obtained at a voltage of −3 V. At these voltages the contrast is mainly caused by topographic effects due to strain induced surface relaxation.[22] The bright contrast corresponds to InAs with the largest lattice constant and the dark contrast is identified as the GaAs interlayer with the smallest lattice constant. From these measurements we determine the height of the dots with bilayer (BL) precision. Note that in X-STM individual ML cannot be distinguished. Figure 2(a) shows two different dots with heights of 3 and 5 BL and Fig. 2(b) shows a dot with a height of 4 BL, which correspond to heights of 6 ± 1, 10 ± 1, and 8 ± 1 ML, respectively. For more than 50 dots the height was measured and the resulting distribution is shown in Fig. 2(c). The quantum dots best resemble circular disks, as depicted in the inset of Fig. 2(a), and therefore the height of the dot is independent of where the dot is cleaved. The height distribution shows that we have quantum dots with heights varying between 5 and 15 ML, which matches quite well with the nine peaks we observe in the macro-PL. A height of 5 ML would then correspond to dots belonging to macro-PL peak $P1$. Moreover, most dots have a height between 7–9 ML corresponding to the part of the PL spectrum which is most intense ($P3-P5$).

The X-STM images also show that the lateral sizes of the quantum dots are less well defined. The largest diameter found by X-STM is 30 nm and corresponds to the value found by AFM.[22] The GaAs interlayer is not located between the InAs dot and the InP substrate, but the InAs dots are rather embedded in the GaAs layer. Although the GaAs layer suppresses the As/P exchange reaction, the actual role of this layer in the growth of these dots is still a matter of further investigation. There appears to be no strong intermixing of Ga and P inside the quantum dot and therefore we conclude that our dots consist of almost pure InAs. For all the studied dots comparable compositions are found. Furthermore, Figs. 2(a) and 2(b) show that the dot formation preferentially takes place at the step edges introduced by the miscut of the substrate.

III. MAGNETOLUMINESCENCE OF INDIVIDUAL QUANTUM DOTS

A. Experiment

In order to study the PL of individual quantum dots we use an aluminum mask on top of the sample, with openings varying between 500 and 1400 nm. Most measurements have been performed on openings of 1 μm. The excitation is provided by a 635 nm wavelength cw laser diode. We studied quantum dots emitting between 1200 and 1600 nm using a confocal microscopy setup. The PL was analyzed in the Faraday configuration in magnetic fields of up to 10 T aligned

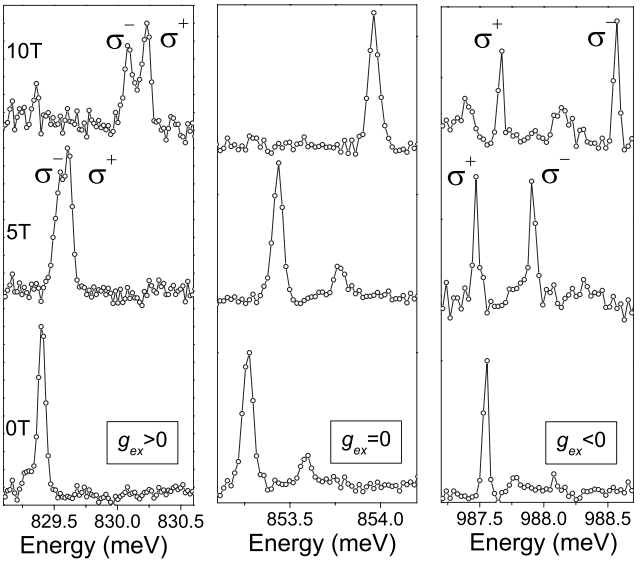

FIG. 3. PL of three individual quantum dots showing from left to right a positive exciton g factor, a quenched g factor, and a negative g factor. The spectra are shown for magnetic fields of 0, 5, and 10 T in the Faraday configuration. The polarization was determined with a quarter lambda plate and a linear polarizer.

parallel with the growth direction.[14,23] The polarization is analyzed using an achromatic quarter-wave plate and a linear polarizer. The luminescence was dispersed by a 75 cm monochromator and detected by an InGaAs array. The linewidth varies from dot to dot, and is of the order of 100 μeV, limited by the quantum dot linewidth itself. In order to exclude biexciton luminescence we performed power-dependent measurements and excluded all lines with a superlinear dependence on the excitation density.[24]

B. Correlation between emission energy, exciton g factor, and diamagnetic shift

The emission energy $E(B)$ of an exciton in a quantum dot in a magnetic field B is in good approximation given by

$$E(B) = E_0 \pm g_{\mathrm{ex}}\mu_B B + \alpha_d B^2, \tag{1}$$

where E_0 is the emission energy at $B=0$ T, $\mu_B = +5.79 \times 10^{-5}$ eV/T is the Bohr magneton, and α_d is the diamagnetic coefficient. The second term of Eq. (1) is the Zeeman term which gives rise to a spin induced splitting of the exciton PL in a magnetic field, whereas α_d is linked to the exciton radius. The magnetoluminescence spectra of three individual quantum dots emitting at different energies are shown in Fig. 3 for magnetic fields of $B=0$, 5, and 10 T. We observe a clear sign change of the polarization of the Zeeman splitted lines for the low-energy quantum dot as compared to the high-energy dot. Moreover, for the quantum dot emitting around 850 meV we observe no Zeeman splitting at all for magnetic fields up to 10 T. All three dots exhibit a diamagnetic shift toward higher energies for increasing magnetic field.

In order to analyze the data we define g_{ex} as

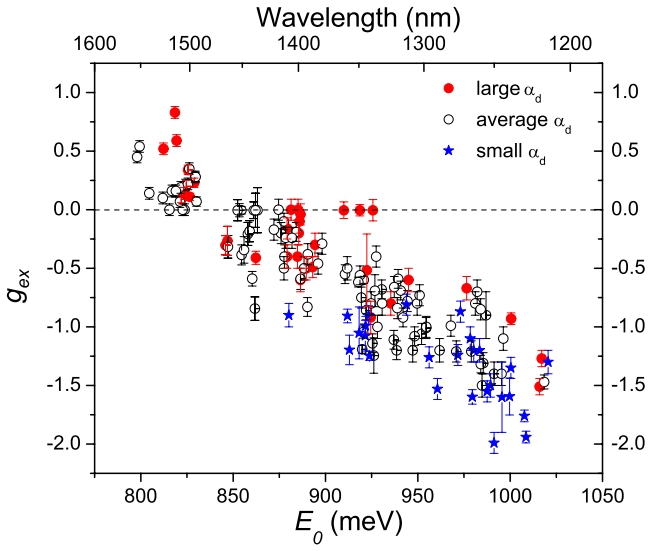

FIG. 4. (Color online) The exciton g factor as function of the emission energy E_0 for 164 quantum dots. A sign change of g_{ex} is observed for dots emitting at low energies. The quantum dots having a small height have a more negative g factor as compared to dots having a large height. Moreover dots having both a small height and a small diamagnetic coefficient α_d (filled blue stars), i.e., small lateral size, have the largest negative g factor. The colors represent different intervals of α_d, and correspond to the colors as shown in the histogram in Fig. 5.

$$g_{\mathrm{ex}} = \frac{E(\sigma^+) - E(\sigma^-)}{\mu_B B}. \tag{2}$$

Figure 3 shows, from left to right, a dot with $g_{\mathrm{ex}} > 0$, $g_{\mathrm{ex}} \simeq 0$, and $g_{\mathrm{ex}} < 0$. In order to verify the sign of g_{ex}, we also measured control samples with known g_{ex} in a given direction of the magnetic field and known angle between the axes of the quarter lambda plate and the linear polarizer. To reveal the relation between g_{ex} and the emission energy we investigated the exciton g factor of in total 164 quantum dots. The dependence of g_{ex} on E_0 is shown in Fig. 4. A strong correlation between E_0 and g_{ex} is observed. At large emission energy the exciton g factor changes its sign and becomes increasingly negative.[25] The exciton g factor changes from +0.5 to −2 for dots emitting at 775–1050 meV. Since the emission energy of the dot is mainly determined by the height of the dot, as is inferred from the macro-PL, the dots having a smaller height have a more negative g_{ex}.

From the magnetic field dependence of the exciton lines we also extract the diamagnetic coefficient α_d, which is to good approximation proportional to the spatial extension of the exciton wave function, and is therefore a measure for the lateral size of the dot.[26] To verify that the emission energy is mainly determined by the height of the dot, we plot α_d against the emission energy in Fig. 5. There is only a weak correlation between emission energy and the diameter of the dots. We therefore conclude that the change from positive to negative values of g_{ex} is governed by the quantum dot height. The weak correlation between E_0 and α_d indicates that dots of smaller (larger) height have on average a smaller (larger) lateral size. Figure 4 shows that quantum dots emitting at the

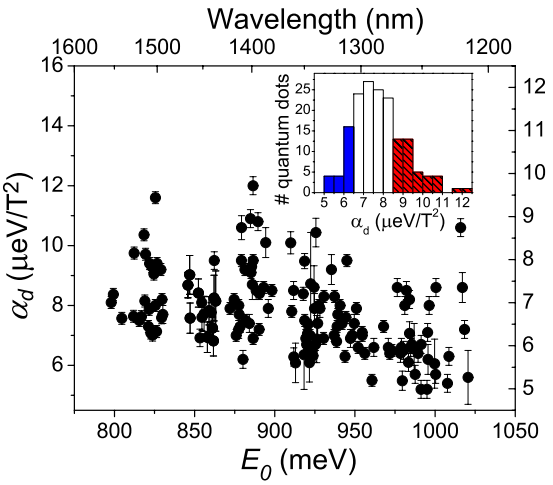

FIG. 5. (Color online) The diamagnetic coefficient as function of the emission energy. There is only a weak correlation between the diamagnetic coefficient and the emission energy. The inset shows the histogram of the different values of α_d. Blue corresponds to small values of α_d, white to the average values of α_d, and red (hatched) to the large values of α_d.

same energy have a large variation in the diamagnetic shift. In order to analyze the importance of the lateral size of the dot on g_{ex}, we specify in Fig. 4 three different ranges of α_d. These ranges are determined from the distribution of α_d as shown in the inset of Fig. 5, and correspond to quantum dots with small (blue), average (white), and large (red) α_d. We find that dots emitting at the same energy, but having a smaller lateral size, have a more negative g_{ex}. Thus reducing the size of the dots, i.e., either height or diameter, will result in more negative values of g_{ex}.

The relation between α_d and g_{ex} is plotted in Fig. 6. We find a strong correlation between α_d and g_{ex}. In general there is an increase in the exciton g factor for increasing α_d. The filled red symbols in the different panels correspond to different emission wavelengths, which correspond to the energy ranges around the peaks in the macro-PL. The filled symbols in the lower right panel correspond to emission energies around peak $P1$ of the macro-PL data and correspond to the dots lowest in height. Quantum dots of the same height, but of smaller diameter, have a more negative g_{ex}. Figure 6 thus shows that quantum dots having the smallest diameter and height, i.e., the overall smallest size, have the most negative g_{ex}. Increasing the size of the dot results in sign change of g_{ex}, where the dots with the overall largest size (filled symbols in the upper left panel) have the most positive g_{ex}.

Up to now we assumed that the change in the emission energy of the dots did not arise from the change in composition of the dots. We can exclude that composition plays a large role as X-STM did not show significant compositional variations over the different dots. Moreover, the influence of the composition on InAs/GaAs dots has been addressed in several papers, which conclude that there is only a small effect on g_{ex}.[8]

To understand the trend toward more negative values of the g_{ex} for smaller dots, we compare our data with the calculations of the electron (g_e) and hole (g_h) g factor for InAs/GaAs quantum dots.[10] The calculations give g_e and g_h as function of increasing emission energy. As the composition is fixed in the calculations, the increase in E_0 is only due to the decreasing size of the quantum dot. The results show that whereas g_e is relatively insensitive for change in the overall size of the dot, there is a strong dependence for g_h on the height and lateral size of the quantum dot. The exciton g factor is defined by $g_{\mathrm{ex}}=-g_e+g_h$. For increasing E_0 (i.e., decreasing size of the dot) the value of g_e increases and g_h decreases, and therefore they both contribute to a more negative g_{ex}. This is in perfect agreement with our experimental observations. Preliminary calculations of the g factors for InAs/InP quantum dots indicate the same trends as for InAs/GaAs quantum dots, although the overall magnitude of the g_h's is smaller.[27] The reduced strain in InAs/InP quantum dots relative to InAs/GaAs quantum dots reduces the splitting of the heavy-hole and light-hole band edges in the dot, and thus there is more light-hole character in the highest-energy hole state of an InAs/InP quantum dot than in that of an InAs/GaAs quantum dot. As the light-hole g factor is less negative than the heavy-hole g factor, this effect leads to less negative g_h's in InAs/InP dots than in InAs/GaAs dots. Smaller dots also have smaller light-hole character in the highest-energy hole state, due to the differing effects of confinement on the heavy- and light-hole energies, and thus smaller quantum dots have more negative g_h's than larger quantum dots, as seen in the measured g_{ex} trend.

C. Anisotropy splitting

Analysis of the single dot spectra showed anisotropy splittings (ΔE_{as}) for 24 quantum dots with a magnitude of up to 250 μeV in zero magnetic field. The measured values of ΔE_{as} are comparable with those found for InAs/GaAs quantum dots.[14] As an example a contour plot of the magnetoluminescence of a quantum dot with $\Delta E_{\mathrm{as}}=160$ μeV is shown in Fig. 7(a). Recently, there has been discussion about the origin of this splitting,[28] but it is generally believed to arise from the asymmetry of the footprint of the dot.[29–31] To demonstrate the dependence of ΔE_{as} on the quantum dot size, we plot ΔE_{as} as a function of the emission energy in Fig. 7(b). In this analysis we only treat the subset of quantum dots that exhibit an anisotropy splitting resolved in our experiments. As shown in Fig. 7(b), dots having a smaller height, i.e., larger E_0, have in general a larger anisotropy splitting. We believe this is due to the fact that for quantum dots of lower height the exciton wave functions are more squeezed in the lateral directions. Therefore they are more sensitive to the asymmetry of the footprint of the dot, resulting in larger values of ΔE_{as}. Nevertheless, higher dots are still sensitive to the confinement potential asymmetries when they have a large lateral size. This is depicted in Fig. 7(b) by making a distinction between dots which have a small and large α_d. The anisotropy splitting for the higher dots is only observed for dots having a large diamagnetic coefficient ($\alpha_d > 7$ μeV/T^2). In general we find that both small and large lateral sizes give rise to an anisotropy splitting for quantum dots of lower height. It should be noticed that the anisotropy splitting does not occur for the negatively and positively

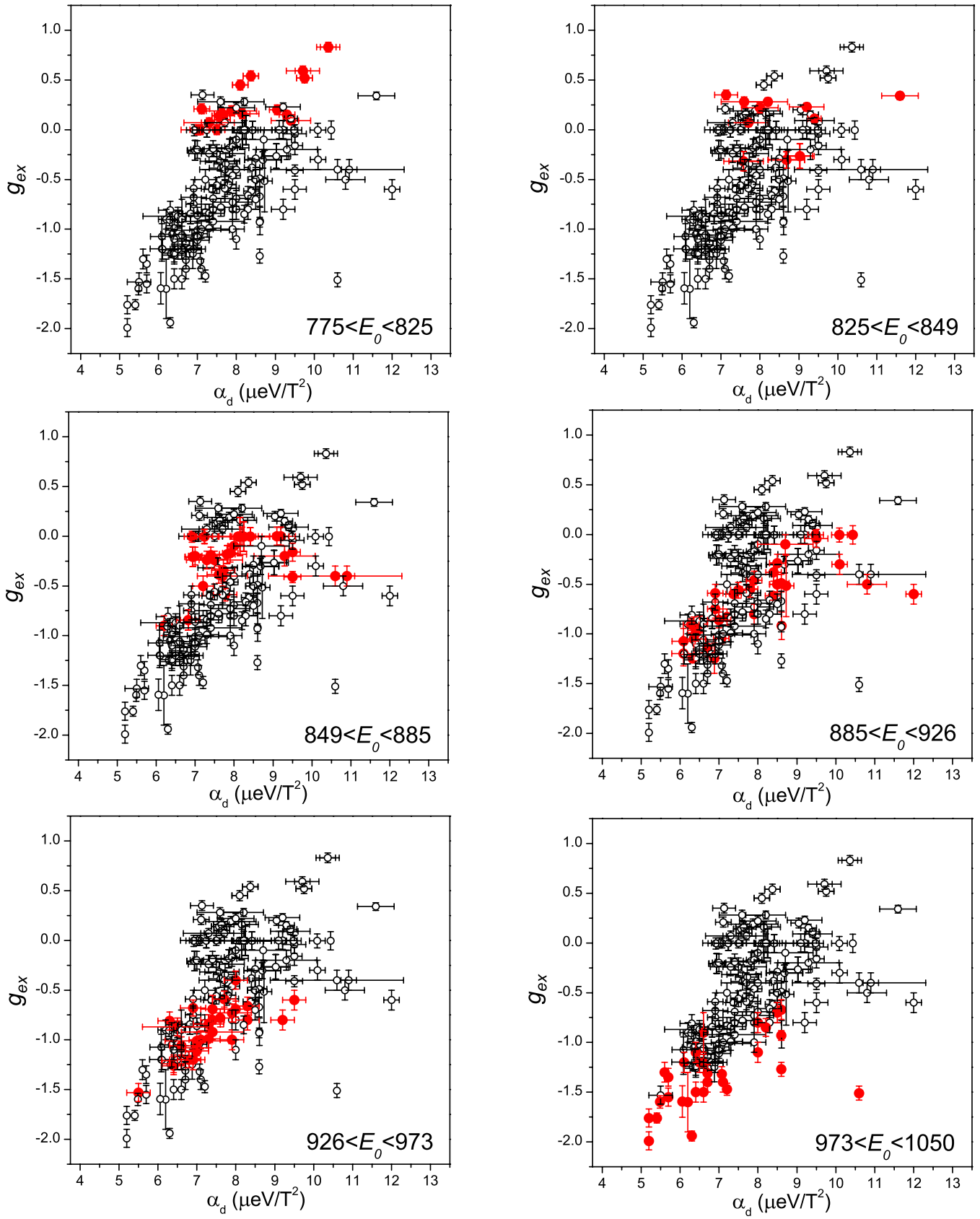

FIG. 6. (Color online) The exciton g factor as function of the diamagnetic coefficient for different emission energies E_0. There is a strong correlation between α_d and g_{ex}. The filled red symbols correspond to the emission range indicated in separate graphs. These emission intervals correspond to the discrete peaks $P1-P6$ in the macro-PL spectrum and thus to dots of different height. The lowest dots which have a smallest lateral size have the most negative exciton g factor.

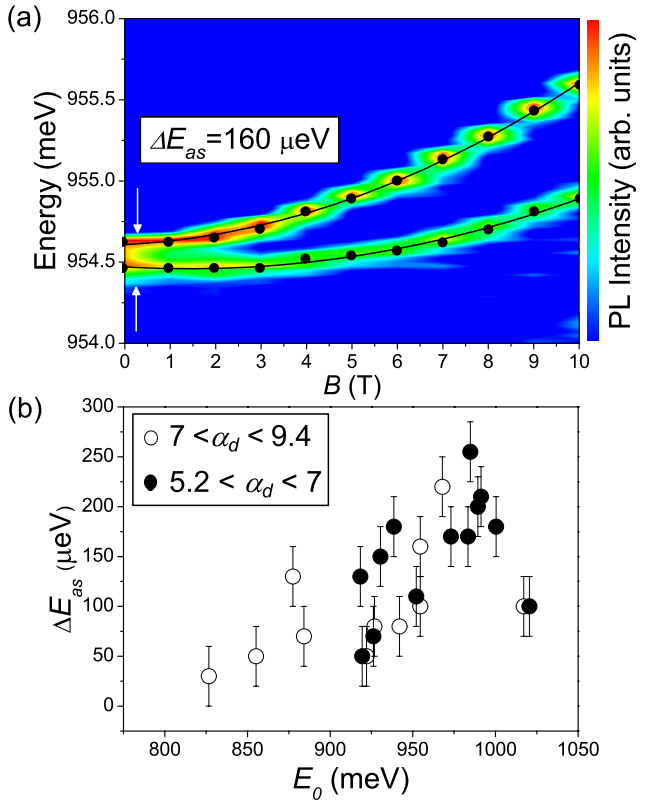

FIG. 7. (Color online) (a) Contour plot of the magnetoluminescence of a dot showing an anisotropy splitting of $\Delta E_{as}=160$ μeV at $B=0$ T. The blue (white) color corresponds to low (high) PL intensity. The peak positions used in the fitting procedure are indicated with the circles and are fitted by the lines using Eq. (1). For this particular dot $g_{ex}=(-1.00\pm0.09)$ and $\alpha_d=(7.1\pm0.2)$ μeV/T^2. (b) The anisotropy splitting ΔE_{as} of in total 24 quantum dots as a function of their emission energy E_0. The filled (empty) circles indicate dots having a small (large) diamagnetic coefficient.

charged excitons, which supports our assumption that we are considering the neutral exciton.

IV. CONCLUSIONS

Macro-PL and X-STM measurements showed that the studied InAs/InP dots have a multimodal height distribution. Single quantum dot luminescence, carried out on a large number of dots, showed a strong correlation between exciton g factor, diamagnetic coefficient, and emission energy. The strong dependence of g_{ex} on the emission energy results in a sign change of the exciton g factor. The trend in g_{ex} is mainly governed by the height variation. We also demonstrated that the value of g_{ex} is correlated with the diamagnetic coefficient and conclude that dots with a large diameter have a smaller g_{ex}. In general dots having a smaller overall size will have a more negative g_{ex} as compared to quantum dots of larger overall size, which is in agreement with calculations performed in Ref. 10. We also showed that for several quantum dots the exciton g factor is quenched. This opens the possibility of evenly tuning the sign of g_{ex} by using for instance electric fields.

We observed anisotropy splittings for InAs/InP quantum dots, and demonstrated that low dots can give rise to a larger anisotropic splitting. We conclude that quantum dots with large height and small lateral size are the most suitable candidates to be used as an entangled photon source since this application relies on dots having small anisotropy splittings.[1] Our study gives a detailed insight into the exciton g factor in quantum dots and opens the possibility of engineering and controlling the g factor in individual quantum dots.

ACKNOWLEDGMENTS

The authors would like to thank T. E. J. Campbell Ricketts for fruitful discussions. This work was part of the research program of NanoNed and FOM, which are financially supported by the NWO (The Netherlands). M.E.F. also acknowledges support from an ONR MURI.

*n.a.j.m.kleemans@tue.nl

[1] R. M. Stevenson, R. J. Young, P. Atkinson, K. Cooper, D. A. Ritchie, and A. J. Shields, Nature (London) **439**, 179 (2006).
[2] D. Loss and D. P. DiVincenzo, Phys. Rev. A **57**, 120 (1998).
[3] S. A. Wolf, D. D. Awschalom, R. A. Buhrman, J. M. Daughton, S. von Molnár, M. L. Roukes, A. Y. Chtchelkanova, and D. M. Treger, Science **294**, 1488 (2001).
[4] M. F. Doty, M. Scheibner, I. V. Ponomarev, E. A. Stinaff, A. S. Bracker, V. L. Korenev, T. L. Reinecke, and D. Gammon, Phys. Rev. Lett. **97**, 197202 (2006).
[5] B. Kane, Nature (London) **393**, 133 (1998).
[6] R. Vrijen, E. Yablonovitch, K. Wang, H. W. Jiang, A. Balandin, V. Roychowdhury, T. Mor, and D. DiVincenzo, Phys. Rev. A **62**, 012306 (2000).
[7] D. Klauser, W. A. Coish, and D. Loss, Adv. Solid State Phys. **46**, 17 (2007).
[8] T. Nakaoka, T. Saito, J. Tatebayashi, and Y. Arakawa, Phys. Rev. B **70**, 235337 (2004).
[9] T. Nakaoka, T. Saito, J. Tatebayashi, S. Hirose, T. Usuki, N. Yokoyama, and Y. Arakawa, Phys. Rev. B **71**, 205301 (2005).
[10] C. E. Pryor and M. E. Flatté, Phys. Rev. Lett. **96**, 026804 (2006); note that the correct trends of the electron and hole g factor are given in the erratum **99**, 179901(E) (2007).
[11] W. Sheng and A. Babinski, Phys. Rev. B **75**, 033316 (2007).
[12] W. Sheng, Physica E (Amsterdam) **40**, 1473 (2008).
[13] G. Medeiros-Ribeiro, E. Ribeiro, and H. Westfahl, Appl. Phys. A: Mater. Sci. Process. **77**, 725 (2003).
[14] M. Bayer, G. Ortner, O. Stern, A. Kuther, A. A. Gorbunov, A. Forchel, P. Hawrylak, S. Fafard, K. Hinzer, T. L. Reinecke, S. N. Walck, J. P. Reithmaier, F. Klopf, and F. Schäfer, Phys. Rev. B **65**, 195315 (2002).
[15] Q. Gong, R. Nötzel, P. J. van Veldhoven, T. J. Eijkemans, and J.

H. Wolter, Appl. Phys. Lett. **84**, 275 (2004).
[16] S. Anantathanasarn, R. Nötzel, P. J. van Veldhoven, T. J. Eijkemans, and J. H. Wolter, J. Appl. Phys. **98**, 013503 (2005).
[17] P. J. Poole, J. McCaffrey, R. L. Williams, J. Lefebvre, and D. Chithrani, J. Vac. Sci. Technol. B **19**, 1467 (2001).
[18] N. Chauvin, E. Tranvouez, G. Bremond, G. Guillot, C. Bru-Chevallier, E. Dupuy, P. Regreny, M. Gendry, and G. Patriarche, Nanotechnology **17**, 1831 (2006).
[19] R. Heitz, F. Guffarth, K. Pötschke, A. Schliwa, D. Bimberg, N. D. Zakharov, and P. Werner, Phys. Rev. B **71**, 045325 (2005).
[20] C. Dion, P. Desjardins, N. Shtinkov, M. D. Robertson, F. Schiettekatte, P. J. Poole, and S. Raymond, Phys. Rev. B **77**, 075338 (2008).
[21] J. M. Ulloa, P. M. Koenraad, E. Gapihan, A. Létoublon, and N. Bertru, Appl. Phys. Lett. **91**, 073106 (2007).
[22] D. M. Bruls, J. W. A. M. Vugs, P. M. Koenraad, H. W. M. Salemink, J. H. Wolter, M. Hopkinson, M. S. Skolnick, Fei Long, and S. P. A. Gill, Appl. Phys. Lett. **81**, 1708 (2002).
[23] C. Schulhauser, D. Haft, R. J. Warburton, K. Karrai, A. O. Govorov, A. V. Kalameitsev, A. Chaplik, W. Schoenfeld, J. M. Garcia, and P. M. Petroff, Phys. Rev. B **66**, 193303 (2002).
[24] A. Chavez-Pirson, J. Temmyo, H. Kamada, H. Gotoh, and H. Ando, Appl. Phys. Lett. **72**, 3494 (1998).
[25] While preparing this paper, an opposite trend of the exciton *g* factor in InAs/InP dots was reported by D. Kim, W. Sheng, P. J. Poole, D. Dalacu, J. Lefebvre, J. Lapointe, M. E. Reimer, G. C. Aers, and R. L. Williams, arXiv:0809.2771v2 (unpublished); up to now we have no understanding of the cause of this opposite trend.
[26] S. N. Walck and T. L. Reinecke, Phys. Rev. B **57**, 9088 (1998).
[27] J. Pingenot, C. E. Pryor, and M. E. Flatté (unpublished).
[28] M. Abbarchi, C. A. Mastrandrea, T. Kuroda, T. Mano, K. Sakoda, N. Koguchi, S. Sanguinetti, A. Vinattieri, and M. Gurioli, Phys. Rev. B **78**, 125321 (2008).
[29] B. Urbaszek, R. J. Warburton, K. Karrai, B. D. Gerardot, P. M. Petroff, and J. M. Garcia, Phys. Rev. Lett. **90**, 247403 (2003).
[30] R. Seguin, A. Schliwa, S. Rodt, K. Pötschke, U. W. Pohl, and D. Bimberg, Phys. Rev. Lett. **95**, 257402 (2005).
[31] J. J. Finley, D. J. Mowbray, M. S. Skolnick, A. D. Ashmore, C. Baker, A. F. G. Monte, and M. Hopkinson, Phys. Rev. B **66**, 153316 (2002).